

Colour Clusters for Computer Diagnosis of Melanocytic Lesions

Stefania Seidenari^a Costantino Grana^b Giovanni Pellacani^a

Departments of ^aDermatology and ^bComputer Engineering, University of Modena and Reggio Emilia, Modena, Italy

Key Words

Melanoma · Atypical naevus · Epiluminescence microscopy · Automated diagnosis · Diagnostic accuracy · Human evaluation

Abstract

Background: To overcome subjectivity and variability in the interpretation of dermoscopic images, image analysis programs, enabling the numerical description of melanocytic lesion images, have been developed. **Objectives:** Our aim was to assess a method for the description of colours in melanocytic lesion images, based on the subdivision of image colours into red, green and blue clusters. **Methods:** Melanomas and naevi of the test set were described by means of 23 colour clusters previously selected by a training set comprising 369 melanocytic lesion images. The diagnostic performance obtained by this automated method was compared to sensitivity and specificity of diagnosis of 4 dermatologists. **Results:** Colour cluster values significantly differed between melanomas and naevi. Moreover, sensitivity and specificity values of computer diagnosis were similar to those achieved by the dermatologists. **Conclusion:** Our image analysis program based on the assessment of one single parameter has the diagnostic accuracy of dermatologists employing dermoscopy on a regular basis.

Copyright © 2007 S. Karger AG, Basel

Introduction

Dermoscopy is reported to improve the diagnostic accuracy concerning malignant melanoma (MM) by 5–30% compared with simple clinical observation. However, dermoscopic techniques require formal training and skill in image interpretation by so-called pattern analysis [1–3]. To overcome the unavoidable subjectivity and variability in the interpretation of dermoscopic images [4], programs for image analysis, enabling the numerical description of the morphology of pigmented skin lesion images, have been developed [5–13]. These programs assess the geometry, texture, pigmentation and the colours of the lesion in an objective and reproducible way, providing mathematical parameters to be used for lesion discrimination. However, only few papers supply a detailed mathematical definition of the parameters which are extrapolated from the image and the correspondence to visible aspects. In past years we provided a technical description of algorithms suitable for the study of borders [14], hyperpigmented regions or relatively dark areas [15], colour areas [16–18], texture [19] and asymmetry of melanocytic lesions [20], also correlating the mathematical parameters to dermoscopic features. We also calculated the sensitivity and specificity of single parameters, in order to investigate their importance in the diagnostic process.

KARGER

Fax +41 61 306 12 34
E-Mail karger@karger.ch
www.karger.com

© 2007 S. Karger AG, Basel
1018–8665/07/2142–0137\$23.50/0

Accessible online at:
www.karger.com/drm

Costantino Grana
Department of Computer Engineering, University of Modena and Reggio Emilia
Via Vignolese 905/B
IT-41100 Modena (Italy)
Tel. +39 059 205 6265, Fax +39 059 205 6129, E-Mail grana.costantino@unimore.it

We are now presenting a new method for the description of colours in melanocytic lesion images, based on the subdivision of image colours into RGB (red, green and blue) clusters, the selection of colour clusters characteristic of melanocytic lesion images of our database and the description of MM and naevus images by means of the distribution of 23 colour clusters. The aim of our study was to assess the importance of this single colour parameter on the process leading to the diagnosis of MM. To this aim, the diagnostic accuracy deriving from image elaboration by this single parameter was evaluated on a training set of 369 melanocytic lesion images and tested on 243 further lesion images. Since the diagnostic performance may depend on the difficulty degree of the image database, we compared the sensitivity and specificity of computer diagnosis with the performance of 4 dermatologists with a different degree of training and experience.

Materials and Methods

Image Database

The training set consisted in 369 melanocytic lesion images, of which 326 referred to naevi and 43 to consecutive MMs, whereas the test set comprised 200 naevi and 43 consecutive MMs. All lesions had been excised and had undergone histopathological examination. MMs of the test set included 8 in situ MMs; their mean thickness was 0.77 mm.

Equipment and Image Acquisition System

For dermoscopic assessment we employed a digital epiluminescence microscope (Foto Finder, Teach Screen software GmbH, Bad Birnbach, Germany), which consists of a probe, comprising a CCD chip colour video camera with an integrated handle and optics for epiluminescence microscopy, a processing unit and a colour monitor. Optics are set in a removable conic structure with a cylindrical transparent spacer and contact plate at the end, and with 6 bright white LEDs, positioned at the bottom of the structure, for constant illumination of the viewing area. The digitized images offer a spatial resolution of 768×576 pixels and 16 million colours. For epiluminescence observation, a drop of contact medium, such as alcohol in water solution, is applied between the contact plane and the skin, enabling the recognition of subsurface structures. The camera system is calibrated monthly on a set of colour patches with known colour properties (Gretag Machbet® Color Checker Chart), and the resulting colour profile is adjusted on the white test patch, between each patient examination, according to a well-defined procedure [21].

Image Analysis Program for Colour Assessment

Since colours perceived by the human observer are produced by a mixture of pixel values, we performed a summarized representation of colours by quantizing the colour space by means of a set of colour clusters. Each cluster is represented by a parallelepiped

in the RGB colour space, oriented along the axes and described by its minimum and maximum RGB values. This simply means that since every pixel of an image is described by 3 different values, we will consider 2 colours being the same if their value falls in the same range for red, green and blue. As an example, if we want to split RGB values into 4 ranges (0–63, 63–127, 128–191, 192–255) the 2 colours (84,32,201) and (126,11,250) will fall in the same cluster.

The first experiment performed on the training set employed a set of 512 uniformly distributed clusters, which corresponds to a 3 bits per channel description, i.e. 9 bits per pixel. After detection of the lesion border [14], we calculated the colour histogram of the whole image population, by counting the number of lesion pixels inside each colour cluster. For image description only 134 of the 512 clusters were necessary. Subsequently, we compared the colour distribution of MMs and naevi by calculating the difference between the percent presence of each colour cluster. Twenty-three colour clusters, which contributed to the overall distribution difference by more than 1%, were selected. These contained 88% of all lesion colours (fig. 1). For each lesion image the number of pixels belonging to each of the 23 clusters was computed. In order to avoid the influence of the lesion area (which is typically larger in MMs) on the final colour information, the cluster pixel values were divided by the lesion area.

Dermatologists' Evaluation of Lesion Images

The images were evaluated by 4 clinicians with different skills in dermoscopy. One of these was employing dermoscopy on a regular basis, but he had not been involved in the collection of the image database considered in this study. The other 3 examiners were residents and had undergone a 6-month daily training on dermoscopy. The clinicians had no access to the clinical image or to clinical data, but only performed their diagnosis observing the dermoscopic images on a computer screen. Possible answers were: melanoma or non-melanoma.

Comparison between Clinical Evaluation and Computer Assessment

Sensitivity and specificity of computer diagnosis and clinicians were compared.

Statistics

For statistical analysis the SPSS statistical package (release 12.0, 2003; SPSS Inc., Chicago, Ill., USA) was used. As basic statistics, the average percentage of colour areas referring to clusters 1–23 within the lesion area and the percentage of lesions presenting different colour clusters in MM and naevus images belonging to the test set were calculated. The Mann-Whitney test was employed to check differences between colour cluster areas of MM and naevi, whereas the χ^2 test and Fisher exact test were used to assess differences in the proportions of MMs and naevi showing different colour clusters. A p value less than 0.05 was considered significant for each performed statistical test.

To examine the discriminant power of our numerical parameters for differentiating between naevi and melanomas, discriminant analysis was performed on a training set comprising 326 naevi and 43 MMs. Discriminant analysis enables the identification of variables, which are important for distinction among the groups, and develops a procedure for group classification based on a score attribution. A linear combination of independent vari-

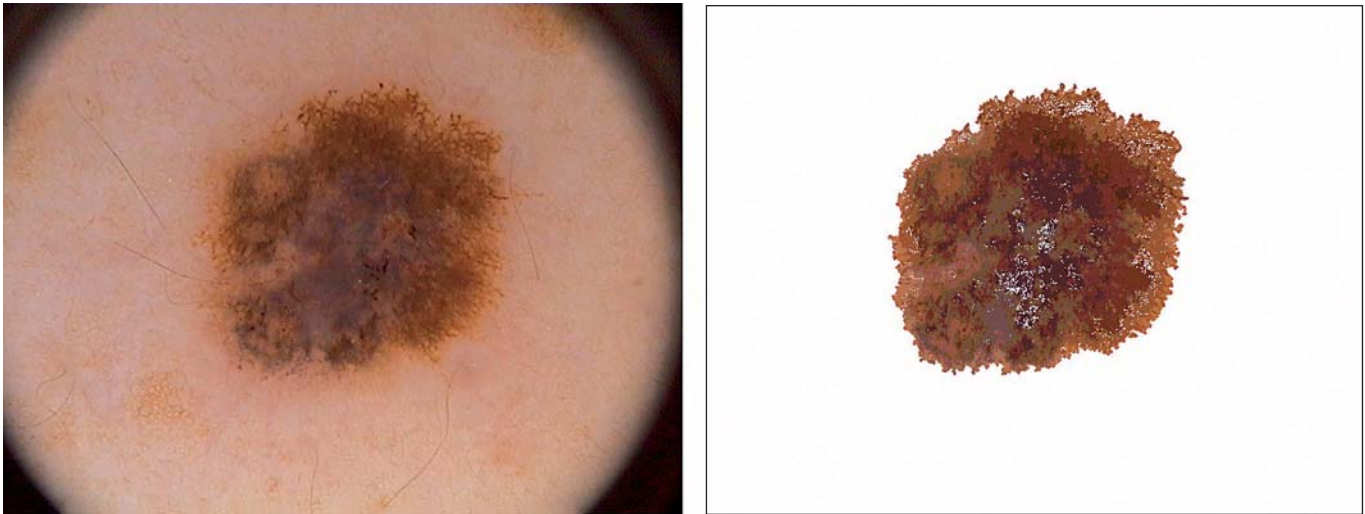


Fig. 1. An MM and the corresponding colour areas. Almost all the image area is covered by the colour clusters selected by our method.

ables is formed and serves as a basis for assigning cases to groups. A D score, obtained for each lesion by the linear discriminant equation, is employed for the attribution of cases to groups. A receiver-operating characteristic analysis was performed to investigate the sensitivity and specificity of the discriminant equation on classification of melanocytic lesions belonging to the test set, comprising the 200 naevi and 43 MMs. Diagnostic accuracy was estimated by the ratio between the percentage of the sum of true positives and true negatives, and the total number of lesions, and was calculated for each threshold (D) value. The area under the curve, which represents an index of the overall discriminant power, and its 95% confidence interval were employed to estimate the likelihood of correctly classifying the lesions into benign and malignant.

Results

All MM images were considered together, and the frequency of each colour in the melanoma population was calculated; the same calculation was performed on naevus images. The 23 colour clusters, showing the largest differences in the percent presence between the MM and naevus populations, were selected and are represented in figure 2. Table 1 lists maximum and minimum RGB values for each of the 23 clusters. Significant differences were observed between the presence of all the 23 colour clusters in the 2 populations of the training set.

On the test set images, we applied the segmentation performed by means of the colour clusters selected on the

training set, thus obtaining the values shown in table 2. Average percentage values of the lesion area occupied by different colour clusters in naevus and MM images showed significant differences for clusters indicated by the asterisks in table 2. Considering a colour cluster present in an image provided that more than half of the average covered area was present, the percentage of lesions presenting different clusters in MM and naevus images significantly differed for colour clusters 1, 3, 4, 7, 12, 19 and 23.

The discriminant analysis procedure applied to the test set enabled the calculation of the area under the curve, which corresponded to a value of 0.810 (95% confidence interval = 0.731–0.888). Moreover, different discriminant analysis D score thresholds were considered, enabling a comparison between the dermatologists' sensitivity and specificity figures and those of the 1-parameter image analysis program. As shown in table 3, setting the D score thresholds to obtain the same sensitivity values achieved by the dermatologists, the corresponding computer specificity values were higher than those of observers No. 1 and 4, lower than that of No. 2 and equal to that of No. 3, whereas considering the same specificity values for the program and the dermatologists, computer sensitivity values were equal to those of 1 and 3, lower than that of 2 and higher in case 4.

Fig. 2. Histograms of the presence of the colours in MM (first bar of the pair) and naevus (second bar of the pair) images of the training set. All MM images were considered together, and the frequency of each colour was calculated; the same calculation was performed on naevus images.

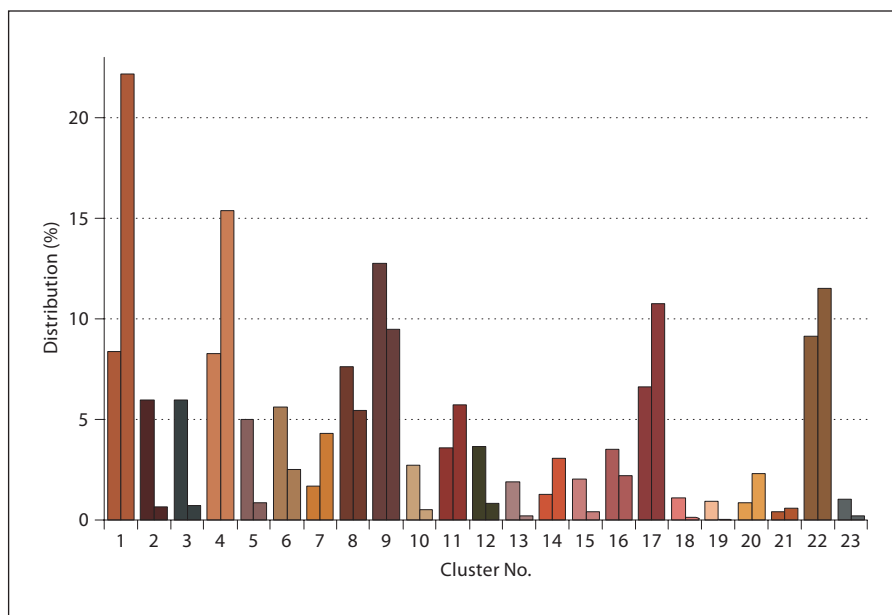



















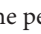


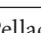


Table 1. Minimum and maximum RGB values of colours used for colour characterization, corresponding colours and percent contribution to the overall colour distribution difference in the training set

Cluster	R _{min}	G _{min}	B _{min}	R _{max}	G _{max}	B _{max}		Difference, %
1	128	64	32	159	95	63		16.57
2	32	0	0	63	31	31		7.48
3	32	32	32	63	63	63		6.62
4	160	96	64	191	127	95		6.07
5	96	64	64	127	95	95		5.65
6	128	96	64	159	127	95		5.04
7	160	96	32	191	127	63		4.61
8	64	32	0	95	63	31		4.26
9	64	32	32	95	63	63		3.58
10	160	128	96	191	159	127		3.42
11	96	32	0	127	63	31		3.05
12	32	32	0	63	63	31		2.98
13	128	96	96	159	127	127		2.68
14	160	64	32	191	95	63		2.61
15	160	96	96	191	127	127		2.27
16	128	64	64	159	95	95		2.24
17	96	32	32	127	63	63		2.02
18	192	96	96	223	127	127		1.50
19	224	160	128	255	191	159		1.19
20	192	128	64	223	159	95		1.12
21	128	64	0	159	95	31		1.08
22	96	64	32	127	95	63		1.07
23	64	64	64	95	95	95		1.06

Colour clusters are listed in the order of values referring to the percent contribution to the overall colour distribution difference.

Table 2. Test set values

Cluster	Colour area of MMs	Colour area of naevi	MMs %	Naevi %
1	10.04*	20.78	53.49*	76.50
2	4.21*	0.52	25.58	15.50
3	4.58*	0.78	27.91*	13.00
4	7.84*	14.21	37.21*	59.00
5	3.54*	0.71	32.56	19.50
6	3.32	2.22	41.86	44.00
7	2.03*	5.02	30.23*	49.50
8	6.16	4.76	41.86	38.00
9	12.07*	8.16	53.49	39.50
10	1.79	0.44	16.28	22.50
11	3.73*	5.33	39.53	49.00
12	2.77*	0.64	34.88*	19.50
13	0.95*	0.31	25.58	4.00
14	1.41*	2.83	30.23	42.50
15	1.88	0.30	30.23	26.00
16	3.07	1.79	39.53	48.50
17	7.07	9.52	53.49	63.00
18	0.87	0.06	16.28	13.50
19	0.72	0.02	4.65*	20.50
20	0.72*	2.73	13.95	29.00
21	0.55*	0.68	25.58	35.00
22	8.85	9.84	58.14	60.50
23	0.69*	0.11	23.26*	7.50

* $p < 0.05$: values found significant by the statistical analysis. Average percentage of colour areas referring to clusters 1-23 within the lesion area (colour area) and percentage of lesions presenting different colours in MM and naevus images belonging to the test set. The colour is considered present in an image only if more than half of the average covered area is present.

Discussion

The assessment of colours is essential for MM diagnosis, both for pattern analysis on dermoscopic images and when employing semiquantitative methods. A blue, red or white colour component is more often present in MMs compared with naevi [16]. Therefore, the detection of these colours within an image may have great diagnostic importance. Moreover, malignant lesions frequently show more than 3 colours, whereas in naevi, 3 or less than 3 colours are usually observed [22]. With the ABCD rule for dermoscopy, the C score, attributed on the basis of the total number of colours of the lesion, contributes approximately to 30% of the final score [1]. According to the Menzies method, the presence of 5–6 colours represents a positive feature for MM diagnosis, whereas a single colour enables the exclusion of the diagnosis of MM [23].

Table 3. Sensitivity (number of MMs correctly identified) and specificity (number of naevi correctly identified) values obtained by the 4 dermatologists and the computer by setting different threshold levels on the discriminant analysis D score

	TP	FP	TN	FN	Sensitivity	Specificity
Observer						
1	29	35	165	14	67.4	82.5
2	34	69	131	9	79.1	65.5
3	28	30	170	15	65.1	85.0
4	27	50	150	16	62.8	75.0
D score threshold						
0.37	29	33	167	14	67.4	83.5
-0.054	34	76	124	9	79.1	62.5
0.4	28	30	170	15	65.1	85.0
0.49	27	29	171	16	62.8	85.5
0.35	29	35	165	14	67.4	82.5
-0.013	33	69	131	10	76.7	65.5
0.64	28	30	170	15	65.1	85.0
0.15	30	50	150	13	69.8	75.0

TP = True positive; FP = false positive; TN = true negative; FN = false negative.

Finally, according to the new 7-point check list, the presence of some colour structures, such as grey-blue areas and regression or scar-like depigmentation, appears relevant for melanoma diagnosis [24].

Due to its diagnostic importance, the analysis of lesion colours has been undertaken by many research groups. One of the most common approaches is to derive basic statistics of colour properties in RGB or other colour spaces. Mean, standard deviation and other simple measures are computed for colours occurring in the lesion and in the surrounding skin, providing colour-related quantitative parameters for subsequent lesion classification [9, 11, 12, 25–30].

According to Binder et al. [10], the number and range of different colours in a reduced colour model represent one of the most important variables for automatic classification. RGB average decile and quartile values were employed by us and were included in the equation for discriminant analysis classification [9, 11]. The image analysis program employed by Rubegni et al. [31] evaluates colour islands including extension and imbalance of so-called peripheral dark regions, i.e. dark, green, green dominant, blue-grey and transition areas. The same group found that 3 variables related to a multicomponent pattern (RGB multicomponent) were significant for differentiating in situ melanomas and atypical naevi [12].

Day and Barbour [32] employed a colour variance parameter in the $L^*a^*b^*$ colour space proposed by Umbaugh et al. [33]. The final feature was relative chromaticity green, a feature measuring the average colour difference between the skin and the lesion. This feature had previously been used by Ercal et al. [25]. Ganster et al. [29] considered minimum, maximum, average and variance of the intensity and hue channels, and also 15 significant colours obtained by the median cut colour quantization algorithm of Heckbert [34].

In a previous study on automated image evaluation, we employed a colour palette, formed by manually chosen colour patches, put together on a visual basis to form colour groups, permitting a description of the 6 main melanocytic lesion colours (black, grey-blue, white, dark brown, tan and red) [16]. The method enabled us to objectively document that the number of colours is higher in MMs with respect to naevi, and that black, white and blue-grey are more frequently observable in the former. Moreover, the correlation between clinical and computer evaluation of the colours was excellent indicating that this colour assessment method is a valuable tool for diagnosis. Subsequently, the extension and distribution of different colour areas in naevi and MMs were described by means of parameters correlated to the clinical concepts of regularity and homogeneity [17, 18]. In particular, asymmetry and inhomogeneity of black areas were typical of melanomas, whereas the regular distribution of dark areas (black or dark brown), usually located centrally and surrounded by a homogeneous light brown ring, was more frequently found in naevi. White colour areas appeared characteristic of malignant lesions, and were larger and more unevenly distributed with respect to naevi. The grey-blue component was observed more frequently in MMs compared to naevi and was also more extended and aggregated in the former.

In this study we propose a further method for the description of colours in melanocytic lesion images, based on image segmentation employing colour clusters. Since colours perceived by the human observer are produced by a mixture of pixel values, we performed a summarized representation of colours by subdividing the colour space into colour clusters, i.e. parallelepipeds in the RGB colour space, comprising a set of RGB values. When comparing the colour distribution of MMs and naevi, we found significant differences in the presence of these colour clusters in the 2 populations. Furthermore, the discriminant analysis procedure applied to the image test set evidenced an area-under-the-curve value corresponding to an acceptable diagnostic accuracy. Our image database was

evaluated by 4 dermatologists employing dermoscopy on a regular basis. Sensitivity and specificity values achieved by these evaluators characterize our image database as being composed of difficult to diagnose images; thus, it enables the evaluation of the diagnostic potential of our 1-parameter program. When setting the discriminant analysis D score thresholds to obtain the same sensitivity and specificity values achieved by the dermatologists, the corresponding sensitivity and specificity computer values were better in 3 cases, equal in 2 and worse in 2.

It is generally accepted that the greater the number of dermoscopic features, presumably secondary to local growth abnormalities, the greater the possibility of melanoma [1, 23, 24]. Thus, when evaluating the diagnostic performance of this automated method, one should consider that in this setting lesion colours were assessed by the program as the only parameter for diagnosis, and that the diagnosis deriving from the evaluation of this single parameter was compared to the diagnostic accuracy of clinicians, who had access to the whole lesion image. Moreover, our program provides the assessment of colours regardless of lesion size, which may influence the diagnostic performance as a fundamental determinant of diagnosis, both on a dermoscopic and an automated basis [30]. Of course, the practical value of an automated diagnosis which allows 63–79% sensitivity and 62–85% specificity is quite low, but it can provide another significant tool for a completely automated system which will have the task to merge the information coming from different automatic techniques.

In conclusion, our image analysis program based on the assessment of 1 single parameter (colour clusters) has the diagnostic accuracy of dermatologists employing dermoscopy on a regular basis, and this both demonstrates the validity of our method and points at the diagnostic importance of colour assessment in the diagnosis of MM.

References

- 1 Zalaudek I, Argenziano G, Di Stefani A, Ferrara G, Marghoob AA, Hofmann-Wellenhof R, Soyer HP, Braun R, Kerl H: Dermoscopy in general dermatology. *Dermatology* 2006; 212:7–18.
- 2 Soyer HP, Braun R, Argenziano G: Dermoscopy coming of age. *Dermatology* 2006;212: 266–267.
- 3 Pehamberger H, Binder M, Steiner A, Wolff K: In vivo epiluminescence microscopy: improvement of early diagnosis of melanoma. *J Invest Dermatol* 1993;100:356S–362S.
- 4 Argenziano G, Soyer HP, Chimenti S, Talamini R, Corona R, Sera F, et al: Dermoscopy of pigmented skin lesions: results of a consensus meeting via the internet. *J Am Acad Dermatol* 2003;48:679–693.
- 5 Cascinelli N, Ferrario M, Bufalino R, Zurrida S, Galimberti V, Mascheroni L, et al: Results obtained by using a computerized image analysis system designed as an aid to diagnosis of cutaneous melanoma. *Melanoma Res* 1992;2:163–170.
- 6 Green AC, Martin NG, Pfitzner J, O'Rourke M, Knight N: Computer image analysis in the diagnosis of melanoma. *J Am Acad Dermatol* 1994;31:958–964.
- 7 Hall PN, Claridge E, Morris Smith JD: Computer screening for early detection of melanoma – Is there a future? *Br J Dermatol* 1995; 132:325–338.
- 8 Gutkowitz-Krusin D, Elbaum M, Szwaykowski P, Kopf AW: Can early malignant melanoma be differentiated from atypical melanocytic nevus by in vivo techniques? II. Automatic machine vision classification. *Skin Res Technol* 1997;3:15–22.
- 9 Seidenari S, Pellacani G, Pepe P: Digital videomicroscopy improves diagnostic accuracy for melanoma. *J Am Acad Dermatol* 1998;39: 175–181.
- 10 Binder M, Kittler H, Seeber A, Steiner A, Pehamberger H, Wolff K: Epiluminescence microscopy-based classification of pigmented skin lesions using computerized image analysis and an artificial neural network. *Melanoma Res* 1998;8:261–266.
- 11 Seidenari S, Pellacani G, Giannetti A: Digital videomicroscopy and image analysis with automatic classification for detection of thin melanomas. *Melanoma Res* 1999;9:163–171.
- 12 Andreassi L, Perotti R, Rubegni P, Burrioni M, Cevenini G, Biagioli M, et al: Digital dermoscopy analysis for the differentiation of atypical nevi and early melanoma. *Arch Dermatol* 1999;135:1459–1465.
- 13 Pellacani G, Martini M, Seidenari S: Digital videomicroscopy with image analysis and automatic classification as an aid for diagnosis of Spitz nevus. *Skin Res Technol* 1999;5: 266–272.
- 14 Grana C, Pellacani G, Cucchiara R, Seidenari S: A new algorithm for border description of polarized light surface microscopic images of pigmented skin lesions. *IEEE Trans Med Imaging* 2003;22:959–964.
- 15 Pellacani G, Grana C, Cucchiara C, Seidenari S: Automated extraction and description of dark areas in surface microscopy melanocytic lesion images. *Dermatology* 2004; 208:21–26.
- 16 Seidenari S, Pellacani G, Grana C: Computer description of colours in dermoscopic melanocytic lesion images reproducing clinical assessment. *Br J Dermatol* 2003;149:523–529.
- 17 Pellacani G, Grana C, Cucchiara R, Seidenari S: Automated description of colours on surface microscopic images of melanocytic lesions. *Melanoma Res* 2004;14:125–130.
- 18 Seidenari S, Pellacani G, Grana C: Colors in atypical nevi: a computer description reproducing clinical assessment. *Skin Res Technol* 2005;11:36–41.
- 19 Seidenari S, Pellacani G, Grana C: Pigment distribution in melanocytic lesion images: a digital parameter to be employed for computer-aided diagnosis. *Skin Res Technol* 2005;11:236–241.
- 20 Seidenari S, Pellacani G, Grana C: Asymmetry in dermoscopic melanocytic lesion images: a computer description based on colour distribution. *Acta Derm Venereol* 2006;86: 123–128.
- 21 Grana C, Pellacani G, Seidenari S, Cucchiara R: Color calibration for a dermatological video camera system. *Proc IAPR Int Conf Pattern Recognition*, Cambridge, UK, 2004, pp 798–801.
- 22 MacKie RM, Fleming C, McMahon AD, Jarret P: The use of the dermatoscope to identify early melanoma using the three-colour test. *Br J Dermatol* 2002;146:481–484.
- 23 Menzies SW, Ingvar C, McCarthy WH: A sensitivity and specificity analysis of the surface microscopy features of invasive melanoma. *Melanoma Res* 1996;6:55–62.
- 24 Argenziano G, Fabbrocini G, Carli P, et al: Epiluminescence microscopy for the diagnosis of doubtful melanocytic skin lesions: comparison of the ABCD rule of dermoscopy and a new 7-point checklist based on pattern analysis. *Arch Dermatol* 1998;134: 1563–1570.
- 25 Ercal F, Chawla A, Stoecker WV, et al: Neural network diagnosis of malignant melanoma from color images. *IEEE Trans Biomed Eng* 1994;9:837–844.
- 26 Cotton SD, Claridge E: Developing a predictive model of human skin coloring. *Proc SPIE Med Imaging Phys Med Imaging* 1996; 2708:814–825.
- 27 Aitken JF, Pfitzner J, Battistutta D, et al: Reliability of computer image analysis of pigmented skin lesions of Australian adolescents. *Cancer* 1996;78:252–257.
- 28 Menzies SW: Automated epiluminescence microscopy: human vs machine in the diagnosis of melanoma. *Arch Dermatol* 1999; 135:1538–1540.
- 29 Ganster H, Pinz A, Rohrer R, et al: Automated melanoma recognition. *IEEE Trans Med Imaging* 2001;20:233–239.
- 30 Kahofer P, Hoffmann-Wellenhof R, Smolle J: Tissue counter analysis of dermoscopic images of melanocytic skin tumors: preliminary findings. *Melanoma Res* 2002;12:71–75.
- 31 Rubegni P, Burrioni M, Sbrano P, Andreassi L: Digital dermoscopy analysis and internet-based program for discrimination of pigmented skin lesion dermoscopic images. *Br J Dermatol* 2005;152:395–396.
- 32 Day GR, Barbour RH: Automated skin lesion screening – A new approach. *Melanoma Res* 2001;11:31–35.
- 33 Umbaugh SE, Moss RH, Stoecker WV, Hance GA: Automatic color segmentation algorithms – with application to skin tumor feature identification. *IEEE Eng Med Biol* 1993; 9:75–82.
- 34 Heckbert P: Color image quantization for frame buffer display. *Comput Graph* 1982; 16:297–307.